^{1}H, ^{13}C, ^{15}N backbone assignment of the human heat-labile enterotoxin B-pentamer and chemical shift mapping of neolactotetraose binding

Daniel Hatlem[1,2], Julie E. Heggelund[1], Daniel Burschowsky[1], Ute Krengel[1], Per E. Kristiansen[2]

[1]Department of Chemistry, University of Oslo, P.O. box 1033 Blindern, 0315 Oslo, Norway

[2]Department of Biosciences, University of Oslo, P.O. box 1066 Blindern, 0316 Oslo, Norway

*Corresponding authors: U Krengel, Tel.: +47 22 85 5461, E-mail: ute.krengel@kjemi.uio.no and PE Kristiansen, Tel.: +47 22856609, E-mail: p.e.kristiansen@ibv.uio.no

Abstract

The major virulence factor of enterotoxigenic *Escherichia coli* (ETEC) is the heat-labile enterotoxin (LT), an AB_5 toxin closely related to the cholera toxin. LT consists of six subunits, the catalytically active A-subunit and five B-subunits arranged as a pentameric ring (LTB), which enable the toxin to bind to the epithelial cells in the intestinal lumen. LTB has two recognized binding sites; the primary binding site is responsible for anchoring the toxin to its main receptor, the GM_1-ganglioside, while the secondary binding site recognizes blood group antigens. Herein, we report the ^{1}H, ^{13}C, ^{15}N main chain assignment of LTB from human isolates (hLTB; 103 a.a. per subunit, with a total molecular mass of 58.5 kDa). The secondary structure was predicted based on $^{13}C'$, $^{13}C^{\alpha}$, $^{13}C^{\beta}$, $^{1}H^{N}$ and ^{15}N chemical shifts and compared to a published crystal structure of LTB. Neolactotetraose (NEO) was titrated to hLTB and chemical shift perturbations were measured. The chemical shift perturbations were mapped onto the crystal structure, confirming that NEO binds to the primary binding site of hLTB and competes with GM_1-binding. Our new data further lend support to the hypothesis that binding at the primary binding site is transmitted to the secondary binding site of the toxin, where it may influence the binding to blood group antigens.

Keywords: ETEC; LTB; molecular recognition; neolactotetraose; protein-carbohydrate interactions

Biological context

Enterotoxigenic *Escherichia coli* (ETEC) cause severe diarrhea, affecting millions of people every year, mainly in the developing world (Huilan et al. 1991; Qadri et al. 2005). The major virulence factor of ETEC is the heat-labile enterotoxin (LT), a hexamer belonging to the AB_5 toxin family, which includes the cholera toxin (CT), shiga toxin and pertussis toxin as the most prominent members (Merritt et al. 1995). LT consists of an A-subunit inserted into a doughnut-shaped B-pentamer (LTB) (Sixma et al. 1991). LT is structurally and functionally similar to the cholera toxin (CT), the main virulence factor of *Vibrio cholerae*, with which it shares approximately 82% sequence identity (Heggelund et al. 2015). During infection, the bacteria colonize the intestine and secrete the holotoxins into the intestinal lumen where the B-pentamer is responsible for anchoring the toxin to the GM_1-receptors present on the epithelial cells (Holmgren 1973). Subsequently, the toxins are internalized and transported to the endoplasmic reticulum by retrograde trafficking (Chinnapen et al. 2007; Wernick et al. 2010). Finally, the catalytic A-subunit enters the cytosol, where it activates adenylyl cyclase (Gill et al. 1978), resulting in an efflux of water and ions over the cell membrane, causing diarrhea. Two saccharide binding sites have been identified on the B-pentamers. The primary binding site is located in the grooves between the B-subunits at the "bottom side" of the toxin, facing the cell membrane. This site is responsible for binding to the main receptor of the toxins, the GM_1 ganglioside (Holmgren 1973). The primary binding site of LTB has been shown to be more promiscuous than in CTB by also binding to GM_2, GD_2, GD_1b and glycoconjugates that carry *N*-acetyllactosamine epitopes such as neolactotetraosylceramide, although significantly weaker than GM_1 (Holmgren et al. 1985; Fukuta et al. 1988; Teneberg et al. 1994; Ångström et al. 1994; MacKenzie et al. 1997; Holmner et al. 2011). The secondary binding site is located at the lateral side of the B-pentamer and binds to blood group antigens (Holmner et al. 2004; Holmner et al. 2007). It is believed that this interaction interferes with the toxin delivery mechanism, thus explaining why individuals with blood group O experience more severe symptoms (Holmner et al. 2004; Harris et al. 2005; Holmner et al. 2007; Heggelund et al. 2012; Mandal et al. 2012; Vasile et al. 2014; Heggelund et al. 2016). A third, putative binding site, to *E. coli* K-12 lipopolysaccharides (LPS), is believed to overlap with the secondary binding site of the toxin (Horstman et al. 2004; Mudrak et al. 2009). The interaction between LPS and LT is thought to have an antagonistic effect on blood-group antigen binding and may explain why ETEC-induced diarrhea does not differ depending on the blood group (Holmner et al. 2007; Holmner et al. 2011).

The B-pentamers play an essential role in the delivery and internalization of LT and CT. In the past 20 years much progress was made in the understanding of their binding properties with regards to GM_1 and blood-group antigen binding (Mudrak et al. 2010; Heggelund et al. 2015). However, the biological significance of the greater promiscuity of the LTB primary binding site and LPS binding

has yet to be explained. In order to identify and study the interactions between the hLTB and its binding partners, we assigned the protein backbone chemical shifts. A secondary structure prediction has been made based on ^{1}H, ^{13}C, ^{15}N-chemical shifts, and subsequently validated by comparing the results with the crystal structure of hLTB (PDB-ID: 2O2L, Holmner et al. 2007). Finally, the chemical shift perturbations of hLTB in complex with neolactotetraose (Galβ4GlcNAcβ3Galβ4Glc; NEO) are reported, showing that NEO indeed binds to the primary binding site, as expected from the crystal structure of LTB in complex with this compound (PDB ID: 2XRS, Holmner et al. 2011; here: LTB from porcine isolates, or pLTB).

Methods and experiments

Protein expression and purification

The hLTB-encoding gene, ExtB (UniProt accession number: P0CK94), was cloned into a pMMB66EH vector under the control of a lac operon and transferred to *Vibrio* sp. 60. A *Vibrio* bacterium was chosen as expression host since E. coli LPS binds to secreted hLTB, retaining it on the bacterial surface, while *Vibrio* LPS does not bind to hLTB, thus increasing the yield (Horstman et al. 2004). hLTB overproduction was induced at $OD_{600nm} = 0.6$ by addition of 1 mM IPTG in M9 medium (Green et al. 2012) for 24 or 72 hours depending on the concentration of D_2O. $^{15}NH_4Cl$ was used for isotopic labeling of ^{15}N-hLTB for titration experiments. For uniform ^{2}H, ^{13}C, and ^{15}N isotope labeling, [$^{13}C_6$, $^{2}H_{12}$]-D-glucose (Cortecnet) and $^{15}NH_4Cl$ (Cortecnet) were used as isotope sources in M9 medium containing 99.9% D_2O (Euriso-top) as solvent. *Vibrio* sp. 60 was trained to grow in 99.9% D_2O by growing 5 mL M9 cultures with step-wise increase of D_2O-concentrations (30, 60, 85, 86, 87, 88, 89, 90, 91, 92, 93, 94, 95, 96, 97, 98 and 99%). The cultures were grown to OD_{600nm} 0.6 before 0.5 mL was transferred to the next step. At concentration above 85%, increments larger than 1% resulted in no growth after 48 hours. At 99% D_2O-concentration, the culture was used to inoculate 500 mL isotopically labeled M9 culture and expressed for 72 hours, yielding 5 mg (10 mg/L) uniformly triply labeled hLTB. hLTB is secreted from the bacteria after production and was harvested by pelleting the bacteria at 10,000 × *g* for 45 minutes at 4 °C and collecting the supernatant. hLTB was further purified by applying the supernatant directly to a 5 mL gravity affinity column containing a resin of immobilized galactose, washing twice with 20 mL Phosphate Buffered Saline (PBS)-buffer (137 mM NaCl, 2.7 mM KCl, 10.1 mM Na_2HPO_4, 2 mM NaH_2PO_4, pH 7.2), and eluted by 10 mL PBS containing 300 mM galactose. Galactose was subsequently removed by dialyzing against PBS overnight. Hydrogen-deuterium exchange of backbone amide hydrogens was performed overnight by dissolving the protein in 6 M guanidine hydrochloride (GndHCl), 5 mM mercaptoethanol, pH 8. The protein was refolded by overnight dialysis against NMR-buffer (50 mM NaCl, 13 mM Na_2HPO_4, 2 mM NaH_2PO_4, 0.02% NaN_3, pH 6.5) containing 1.5 mM reduced and oxidized glutathione (1:1) and 0.5 M GndHCl. The refolded protein was subsequently dialyzed 3 times against NMR-buffer to

remove any residual GndHCl and concentrated using a 10 kDa MWCO centrifugal filter (Amicon, Sigma-Aldrich).

NMR spectroscopy and data processing

NMR experiments for backbone assignment were carried out in a D_2O matched 5 mm Shigemi tube containing 280 µL 1 mM triply labeled hLTB in NMR buffer (described above) containing 7% D_2O, 0.2 mM 4,4-dimethyl-4-silapentanesulfonic acid (DSS). Spectra were acquired at 308 K on a Bruker Avance II 600 MHz NMR spectrometer equipped with a 5mm $^{1}H/^{13}C/^{15}N$-cryoprobe. For the assignment, the following spectra were collected: ^{15}N-^{1}H-TROSY, TROSY-HNCO, TROSY-HN(CA)CO, TROSY-HNCA, TROSY-HN(CO)CA, TROSY-HNCACB and TROSY-HN(CO)CACB (Salzmann et al. 1999). The spectra were processed using TopSpin version 1.3/2.6 and all peaks were picked and assigned in Cara 1.8.4.2 (Keller 2004). DSS was used as a chemical shift standard, and ^{13}C and ^{15}N data were referenced using frequency ratios as previously described (Wishart et al. 1995). Chemical shift values were exported to Talos+ web client for chemical shift indexing (Wishart et al. 1994; Shen et al. 2009). Titration experiments with ^{15}N labeled hLTB were carried out under the same conditions with 400 µL sample in a 5 mm thin wall Wilmad NMR tube. The initial ^{15}N-^{1}H-TROSY spectrum was collected at a NEO:hLTB ratio of 0.25:1, and then increased step-wise to 200:1. Averaged chemical shift perturbations were calculated from the changes observed in chemical shifts between the NEO:hLTB 0:1 and NEO:hLTB 200:1 spectrum using the formula:

$\Delta\delta = \sqrt{\Delta\delta(^{1}\mathrm{H})^2 + \frac{1}{5}(\Delta\delta(^{15}\mathrm{N}))^2}$ (Schumann et al. 2007).

Assignment and data deposition

The acquired ^{15}N-TROSY spectrum of hLTB (57.8 kDa) was well resolved, with good dispersion and line shape, as shown in Fig. 1, indicating that the protein is folded and behaves well in solution. Out of 99 non-proline residues, HN-backbone cross peaks, 93 were observable in the ^{15}N-^{1}H-TROSY spectrum. The six unobservable residues, H13, S55, I58-S60 and K63 are all located in loops, indicating that the absence of signal could be caused by intermediary conformational exchange. Following a triple-resonance approach, we can report the assignment of 93 $^{1}H^{N}$ (94%), 93 ^{15}N (94%), 79 $^{13}C'$ (77%), 98 $^{13}C^{\alpha}$ (96%) and 98 $^{13}C^{\beta}$ (96%) main chain nuclei. The TROSY-HNCACB spectrum was generally the most informative of the spectra due to its high signal-to-noise ratio, yielding an almost complete assignment of $^{13}C^{\alpha}$ and $^{13}C^{\beta}$s.

Secondary structure prediction was performed using the Talos+ web client (Wishart and Sykes 1994; Shen et al. 2009) and chemical shift assignments. According to the secondary structure prediction (Fig. 2), hLTB contains two α-helices (I5-C9 and Q61-L77) and six β-sheets (I17-T19, I24-M31, M37-T41, F48-E51, K84-W88 and A98-E102). The secondary structure prediction is in overall good

agreement with the crystal structure (PDB-ID: 2O2L, Holmner et al. 2011), which contains the same number, placement and approximate length of secondary structure elements (Fig. 2). This strongly indicates that the protein adopts the same structure in solution as in the crystal form, and excludes the possibility of gross assignment errors.

Neolactotetraose (NEO) is a secondary receptor present on the surface of small intestinal epithelial cells (Karlsson et al. 1996) that may be competing with GM_1, the primary receptor of LTB. The crystal structure of NEO in complex with LTB from porcine isolates (pLTB) shows that NEO binds in the primary binding site of the toxin (Holmner et al. 2011). However, it has not been confirmed that this is also the case for hLTB (or outside the crystal environment). In the primary binding site, pLTB and hLTB differ by only one residue (H13 in hLTB, R13 in pLTB). This difference may, at least in part, explain the different binding affinities of NEO to hLTB and pLTB (Holmner et al. 2011) (pLTB binds more strongly, as determined from microtiter well assays (Teneberg et al. 1994; Holmner et al. 2011)). To investigate the binding properties of the toxin in solution, NEO was titrated to ^{15}N labeled hLTB in order to measure the chemical shift perturbations (Fig. 3ab). When mapped onto the structure of hLTB, residues showing the greatest chemical shift perturbations, N14, G33, E51, Q56, W88 and N90, are clustered in and around the primary binding site (Fig. 3c and d, colored red and orange), confirming that NEO also in solution binds to the hLTB primary binding site. Even though H13 itself could not be assigned, the surrounding residues experience chemical shift perturbations, indicating that H13 is also involved in binding. An unknown, well-resolved peak at 10.1 ^{1}H-ppm, 124.0 ^{15}N-ppm in the ^{1}H-^{15}N-TROSY during the titration could be caused by a change in the pKa of the H13-imidazole side chain upon NEO binding.

We have earlier hypothesized that NEO or GM_1 binding in the primary binding site may stabilize loop residues 55-60, which may induce structural changes that affect the secondary binding site, for blood group antigens (Holmner et al. 2011). We observed chemical shift changes for residues G54, K62, A64, and I65 in the helix connecting the primary and secondary binding sites upon binding of NEO, supporting this hypothesis. Additionally, residues Q3, S4, Q16, Y18, T47, and F48, which participate in blood group antigen binding (Holmner et al. 2007; Heggelund et al. 2016), as well as W88 and K91 from the primary binding site exhibit peak perturbations, albeit to a lesser extent.

The main chain ^{1}H, ^{15}N, ^{13}C chemical shifts have been deposited in the BioMagnetic Resonance dataBank (BMRB) under deposition number: 26966.

Acknowledgements

We would like to thank the students Aleksandra Suchodolska and Njáll Ekstrøm for their contributions to this project. This work was funded by the University of Oslo and the Norwegian Research Council (Grant 214037).

References

Chinnapen DJ, Chinnapen H, Saslowsky D, Lencer WI (2007) Rafting with cholera toxin: endocytosis and trafficking from plasma membrane to ER. FEMS Microbiol Lett 266:129-137 doi:10.1111/j.1574-6968.2006.00545.x

Fukuta S, Magnani JL, Twiddy EM, Holmes RK, Ginsburg V (1988) Comparison of the carbohydrate-binding specificities of cholera toxin and *Escherichia coli* heat-labile enterotoxins LTh-I, LT-IIa, and LT-IIb. Infect Immun 56:1748-1753

Gill DM, Meren R (1978) ADP-ribosylation of membrane proteins catalyzed by cholera toxin: basis of the activation of adenylate cyclase. Proc Natl Acad Sci U S A 75:3050-3054

Green MR, Sambrook J, Sambrook J (2012) Molecular cloning : a laboratory manual. 4th edn. Cold Spring Harbor Laboratory Press, Cold Spring Harbor, N.Y.

Harris JB, Khan AI, LaRocque RC, Dorer DJ, Chowdhury F et al. (2005) Blood group, immunity, and risk of infection with *Vibrio cholerae* in an area of endemicity. Infect Immun 73:7422-7427 doi:10.1128/IAI.73.11.7422-7427.2005

Heggelund JE, Bjørnestad VA, Krengel U (2015) 7 - *Vibrio cholerae* and *Escherichia coli* heat-labile enterotoxins and beyond. In: Ladant D, Popoff MR (eds) The Comprehensive Sourcebook of Bacterial Protein Toxins (Fourth Edition). Academic Press, Boston, pp 195-229. doi:10.1016/B978-0-12-800188-2.00007-0

Heggelund JE, Burschowsky D, Bjørnestad VA, Hodnik V, Anderluh G, Krengel U (2016) High-resolution crystal structures elucidate the molecular basis of cholera blood group dependence. PLoS Pathog 12:e1005567 doi:10.1371/journal.ppat.1005567

Heggelund JE, Haugen E, Lygren B, Mackenzie A, Holmner A et al. (2012) Both El Tor and classical cholera toxin bind blood group determinants. Biochem Bioph Res Co 418:731-735 doi:DOI 10.1016/j.bbrc.2012.01.089

Holmgren J (1973) Comparison of the tissue receptors for *Vibrio cholerae* and *Escherichia coli* enterotoxins by means of gangliosides and natural cholera toxoid. Infect Immun 8:851-859

Holmgren J, Lindblad M, Fredman P, Svennerholm L, Myrvold H (1985) Comparison of receptors for cholera and *Escherichia coli* enterotoxins in human intestine. Gastroenterology 89:27-35

Holmner Å, Askarieh G, Ökvist M, Krengel U (2007) Blood group antigen recognition by *Escherichia coli* heat-labile enterotoxin. J Mol Biol 371:754-764 doi:10.1016/j.jmb.2007.05.064

Holmner Å, Lebens M, Teneberg S, Ångström J, Ökvist M, Krengel U (2004) Novel binding site identified in a hybrid between cholera toxin and heat-labile enterotoxin: 1.9 Å crystal structure reveals the details. Structure 12:1655-1667 doi:10.1016/j.str.2004.06.022

Holmner Å, Mackenzie A, Ökvist M, Jansson L, Lebens M, Teneberg S, Krengel U (2011) Crystal structures exploring the origins of the broader specificity of E*scherichia coli* heat-labile enterotoxin compared to cholera toxin. J Mol Biol 406:387-402 doi:10.1016/j.jmb.2010.11.060

Horstman AL, Bauman SJ, Kuehn MJ (2004) Lipopolysaccharide 3-deoxy-D-manno-octulosonic acid (Kdo) core determines bacterial association of secreted toxins. J Biol Chem 279:8070-8075 doi:10.1074/jbc.M308633200

Huilan S, Zhen LG, Mathan MM, Mathew MM, Olarte J et al. (1991) Etiology of acute diarrhea among children in developing-countries - a multicenter study in 5 countries. B World Health Organ 69:549-555

Karlsson KA, Teneberg S, Ångström J, Kjellberg A, Hirst TR, Berström J, Miller-Podraza H (1996) Unexpected carbohydrate cross-binding by *Escherichia coli* heat-labile enterotoxin. Recognition of human and rabbit target cell glycoconjugates in comparison with cholera toxin. Bioorg Med Chem 4:1919-1928

Keller R (2004) The computer aided resonance assignment tutorial, 1st edn. CANTINA Verlag, Goldau

MacKenzie CR, Hirama T, Lee KK, Altman E, Young NM (1997) Quantitative analysis of bacterial toxin affinity and specificity for glycolipid receptors by surface plasmon resonance. J Biol Chem 272:5533-5538

Mandal PK, Branson TR, Hayes ED, Ross JF, Gavin JA, Daranas AH, Turnbull WB (2012) Towards a structural basis for the relationship between blood group and the severity of El Tor cholera. Angew Chem Int Ed Engl 51:5143-5146 doi:10.1002/anie.201109068

Merritt EA, Hol WGJ (1995) AB5 toxins. Curr Opin Struct Biol 5:165-171

Mudrak B, Kuehn MJ (2010) Heat-labile enterotoxin: beyond G(m1) binding. Toxins (Basel) 2:1445-1470 doi:10.3390/toxins2061445

Mudrak B, Rodriguez DL, Kuehn MJ (2009) Residues of heat-labile enterotoxin involved in bacterial cell surface binding. J Bacteriol 191:2917-2925 doi:10.1128/JB.01622-08

Qadri F, Svennerholm AM, Faruque AS, Sack RB (2005) Enterotoxigenic *Escherichia coli* in developing countries: epidemiology, microbiology, clinical features, treatment, and prevention. Clin Microbiol Rev 18:465-483 doi:10.1128/CMR.18.3.465-483.2005

Salzmann M, Wider G, Pervushin K, Senn H, Wüthrich K (1999) TROSY-type triple-resonance experiments for sequential NMR assignments of large proteins. J Am Chem Soc 121:844-848 doi:Doi 10.1021/Ja9834226

Schumann F, Riepl H, Maurer T, Gronwald W, Neidig K-P, Kalbitzer H (2007) Combined chemical shift changes and amino acid specific chemical shift mapping of protein–protein interactions. J Biomol NMR 39:275-289 doi:10.1007/s10858-007-9197-z

Shen Y, Delaglio F, Cornilescu G, Bax A (2009) TALOS+: a hybrid method for predicting protein backbone torsion angles from NMR chemical shifts. J Biomol NMR 44:213-223 doi:10.1007/s10858-009-9333-z

Sixma TK, Pronk SE, Kalk KH, Wartna ES, van Zanten BA, Witholt B, Hol WGJ (1991) Crystal structure of a cholera toxin-related heat-labile enterotoxin from *E. coli*. Nature 351:371-377 doi:10.1038/351371a0

Teneberg S, Hirst TR, Ångström J, Karlsson KA (1994) Comparison of the glycolipid-binding specificities of cholera toxin and porcine *Escherichia coli* heat-labile enterotoxin: identification of a receptor-active non-ganglioside glycolipid for the heat-labile toxin in infant rabbit small intestine. Glycoconj J 11:533-540

Vasile F, Reina JJ, Potenza D, Heggelund JE, Mackenzie A, Krengel U, Bernardi A (2014) Comprehensive analysis of blood group antigen binding to classical and El Tor cholera toxin B-pentamers by NMR. Glycobiology 24:766-778 doi:10.1093/glycob/cwu040

Wernick NL, Chinnapen DJ, Cho JA, Lencer WI (2010) Cholera toxin: an intracellular journey into the cytosol by way of the endoplasmic reticulum. Toxins (Basel) 2:310-325 doi:10.3390/toxins2030310

Wishart DS, Bigam CG, Yao J, Abildgaard F, Dyson HJ et al. (1995) 1H, 13C and 15N chemical shift referencing in biomolecular NMR. J Biomol NMR 6:135-140

Wishart DS, Sykes BD (1994) The C-13 chemical-shift index - a simple method for the identification of protein secondary structure using C-13 chemical-shift data. J Biomol NMR 4:171-180

Ångström J, Teneberg S, Karlsson KA (1994) Delineation and comparison of ganglioside-binding epitopes for the toxins of *Vibrio cholerae*, *Escherichia coli*, and *Clostridium tetani*: evidence for overlapping epitopes. Proc Natl Acad Sci U S A 91:11859-11863

Figure Captions

Fig. 1 ^{1}H, ^{15}N-TROSY spectrum of triply labeled hLTB. The spectrum was recorded after performing proton exchange and refolding as described in experimental section, recorded at 600 MHz. Backbone assignment of all visible backbone peaks are marked with arrows. The indole ring of W88 and the N103 side chain are also assigned

Fig. 2 Secondary structure assignment. TALOS+ predicted secondary structure of hLTB based on ^{13}C', $^{13}C^{\alpha}$, $^{13}C^{\beta}$, $^{1}H^{N}$ and ^{15}N chemical shifts compared to the secondary structure observed in the crystal structure of hLTB (PDB-ID: 2O2L, Holmner et al. 2007). Ψ-angles, with standard deviation bars, predicted by TALOS+ are plotted below the secondary structures. Blank bars correspond to prolines or unassigned residues.

Fig. 3 Titration experiment with neolactotetraose (NEO). **a** Superimposition of hLTB ^{15}N-TROSY spectra, collected in the absence (red) and presence (blue) of NEO. **b** Bars showing the combined ^{15}N-^{1}H δΔ chemical shift change of hLTB upon binding to NEO. Horizontal lines show the cut-off levels of 0.4 and 0.2 ppm **c** Surface representation of hLTB (PDB-ID: 2O2L, Holmner et al. 2007) superimposed with NEO from the pLTB structure in complex with this ligand (PDB-ID: 2XRS, Holmner et al. 2011). The interacting residues are color coded by extent of chemical shift perturbation upon NEO binding. Red and orange correspond to 0.4 and 0.3 ppm respectively. Residues colored blue are non-proline residues that could not be assigned since the resonances were not visible in the ^{15}N-^{1}H-TROSY spectrum. Representative primary and secondary binding sites are marked with arrows. **d** Close-up view of one of the primary binding sites, viewed from the "bottom side" of the toxin, with docked NEO from the pLTB structure. Only one of the five NEO-binding sites was colored.

Fig. 1

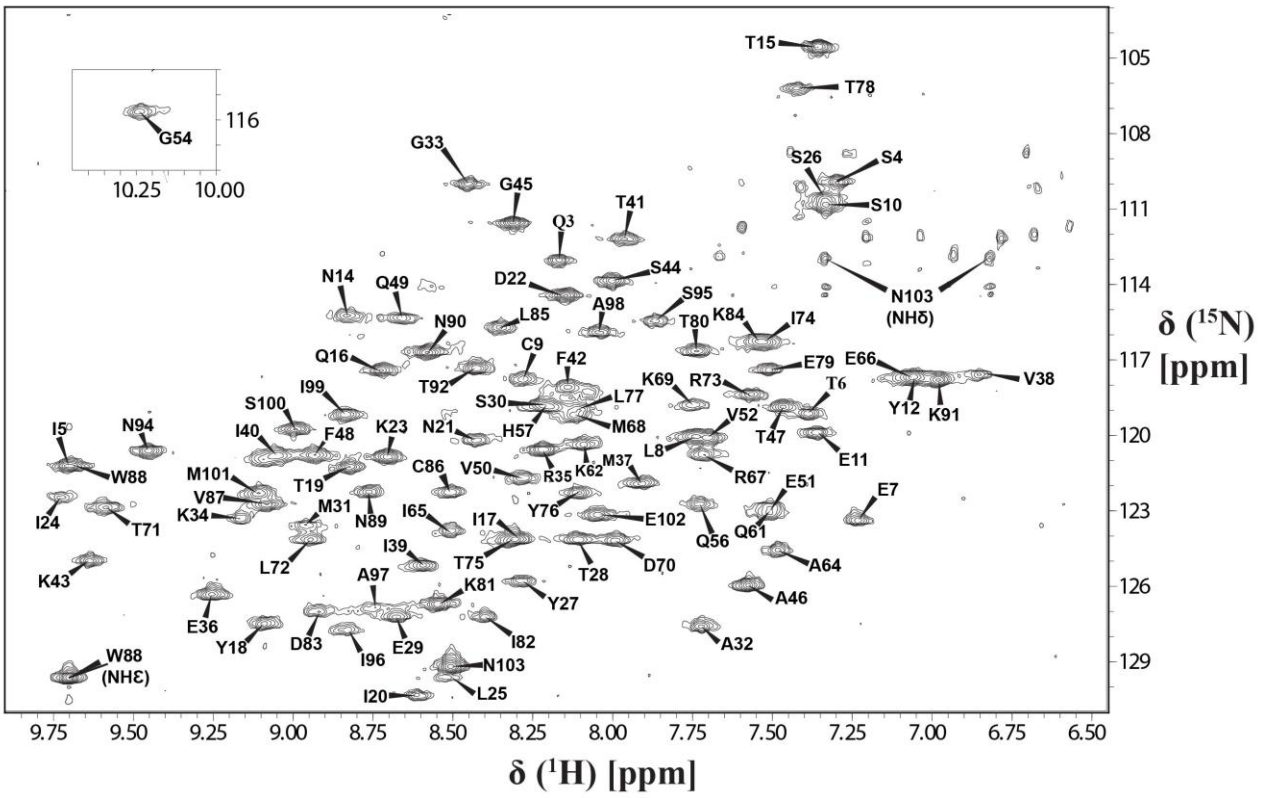
T15
T78
G54
116
10.25
10.00
G33
G45
S26
S4
S10
T41
Q3
N14
Q49
D22
S44
N103
(NHδ)
S95
A98
N90
L85
T80
K84
I74
C9
F42
Q16
T92
E79
E66
V38
I99
K69
R73
T6
S100
S30
L77
Y12
K91
I5
N94
I40
F48
K23
N21
H57
M68
V52
T47
L8
E11
W88
M101
C86
V50
R35
K62
M37
R67
E51
E7
V87
T19
I24
T71
K34
M31
N89
I65
I17
Y76
E102
Q56
Q61
I39
L72
T75
T28
D70
A64
K43
A97
K81
Y27
A46
E36
Y18
D83
E29
I82
A32
I96
N103
W88
(NHε)
I20
L25
105
108
111
114
117
120
123
126
129
δ (15N) [ppm]
9.75
9.50
9.25
9.00
8.75
8.50
8.25
8.00
7.75
7.50
7.25
7.00
6.75
6.50
δ (1H) [ppm]

Fig. 2

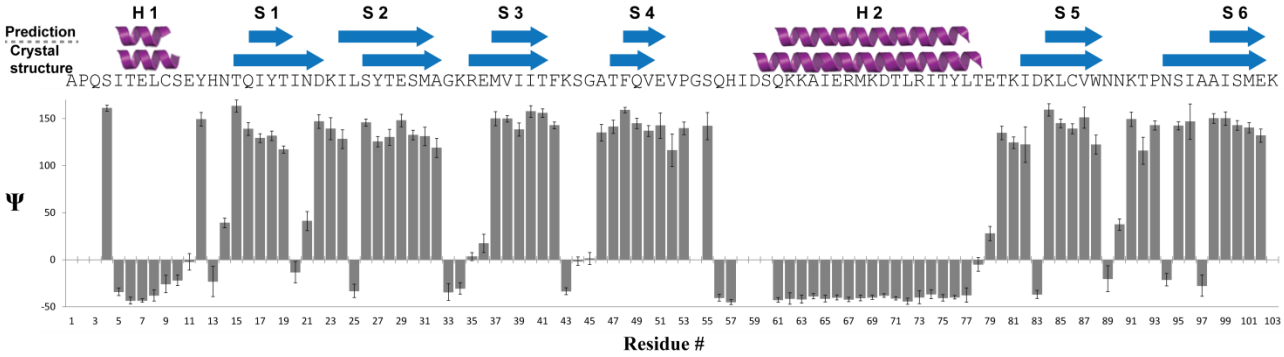
H 1
S 1
S 2
S 3
S 4
H 2
S 5
S 6
Prediction
Crystal structure
APQSITELCSEYHNTQIYTINDKILSYTESMAGKREMVIITFKSGATFQVEVPGSQHIDSQKKAIERMKDTLRITYLTETKIDKLCVWNNKTPNSIAAISMEK
Ψ
150
100
50
0
-50
1 3 5 7 9 11 13 15 17 19 21 23 25 27 29 31 33 35 37 39 41 43 45 47 49 51 53 55 57 59 61 63 65 67 69 71 73 75 77 79 81 83 85 87 89 91 93 95 97 99 101 103
Residue #

Fig. 3

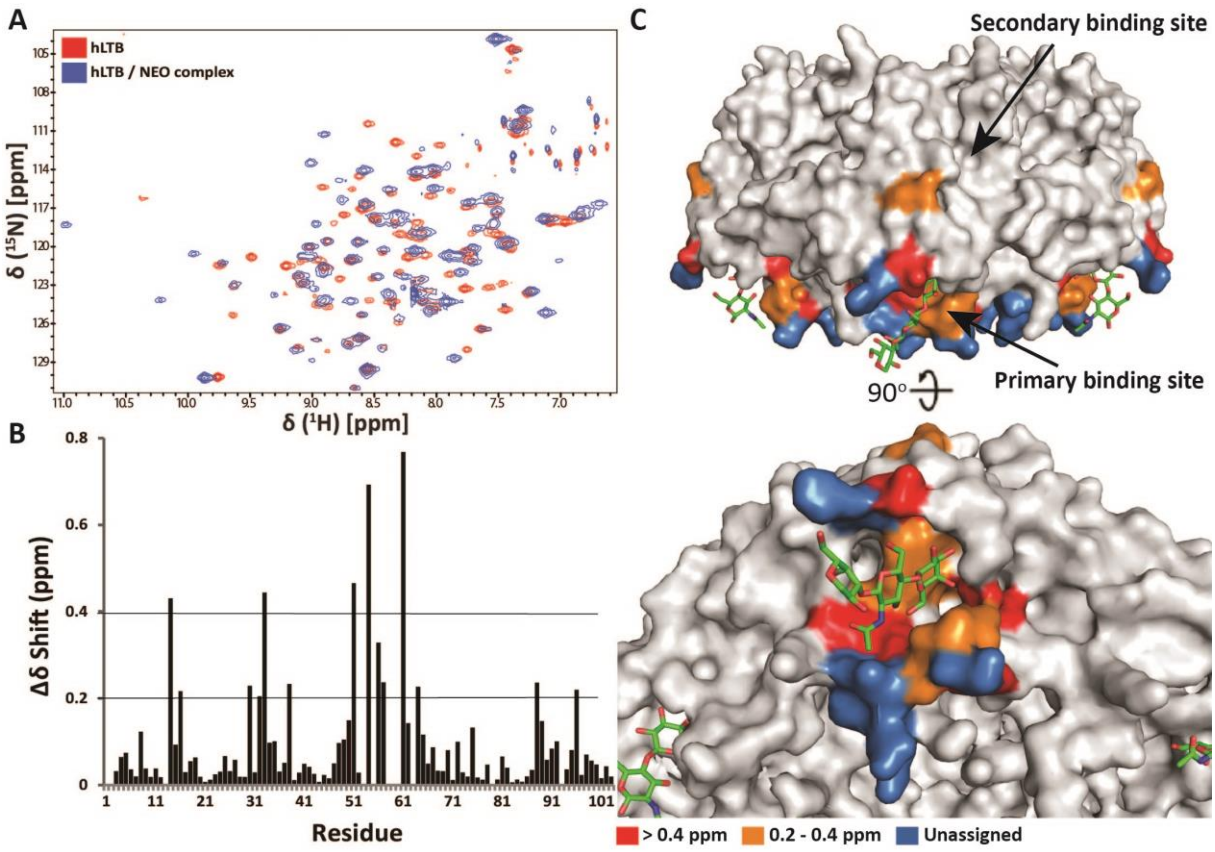
A
hLTB
hLTB / NEO complex
δ (15N) [ppm]
δ (1H) [ppm]
B
Δδ Shift (ppm)
Residue
C
Secondary binding site
Primary binding site
90°
> 0.4 ppm
0.2 - 0.4 ppm
Unassigned